The immersed boundary method: a finite element approach

Daniele Boffi [a], Lucia Gastaldi [b,*]

[a] Dipartimento di Matematica, Università di Pavia, via Ferrata 1, Pavia, Italy
[b] Dipartimento di Matematica, Università di Brescia, via Valotti 9, Brescia, Italy

Abstract

In this paper we consider a modification of the immersed boundary method based on a finite element approximation of the fluid. Besides some theoretical considerations, we present two-dimensional numerical examples which confirm the good behavior of the computed solutions.

Keywords: Immersed boundary method; Finite element method

1. Introduction

The immersed boundary (IB) method was developed for the computer simulation of fluid–structure interaction, especially in biological fluid dynamics (see [1] and the bibliography quoted therein). The coupling of fluids and solids is the central feature in the study of the mechanics of the heart, arteries, veins, micro-circulation, and pulmonary blood flow. The IB method is at the same time a mathematical formulation and a numerical scheme. The mathematical formulation is based on the use of Eulerian variables to describe the dynamic of the fluid and of Lagrangian variables along the moving structure. The force exerted by the structure on the fluid is taken into account by means of a Dirac function constructed according to certain principles. This is a different approach with respect to the conventional one, which consists in separating the system in its two components coupled by boundary conditions (see, e.g. [2–5]).

The original IB method uses finite differences in order to approximate the Navier–Stokes equations. In [6] we introduced a suitable modification of the IB method which makes use of finite elements and gave a first contribution towards the analysis of it. One of the main features of the finite element approach is that in this case there is no need of approximating the Dirac function, as it is usually done with the original finite difference formulation. Indeed, the load term arising by the presence of the boundary in the fluid can be naturally handled in a variational form. In this paper we present some two-dimensional numerical tests which confirm the good behavior of our method.

2. Setting of the problem

We consider the model problem of a viscous incompressible fluid in a two-dimensional square domain Ω containing an immersed massless elastic boundary in the form of a curve. To be more precise, for all $t \in [0,T]$, let Γ_t be a simple closed curve, the configuration of which is given in a parametric form, $\mathbf{X}(s,t)$, $0 \le s \le L$, $\mathbf{X}(0,t) = \mathbf{X}(L,t)$ (see [7,8]). The equations of motion of the system are

$$\rho \frac{\partial \mathbf{u}}{\partial t} - \mu \Delta \mathbf{u} + \mathbf{u} \cdot \nabla \mathbf{u} + \nabla p = \mathbf{F} \quad \text{in } \Omega \times]0,T[\tag{1}$$

$$\nabla \cdot \mathbf{u} = 0 \quad \text{in } \Omega \times]0,T[\tag{2}$$

$$\mathbf{F}(\mathbf{x},t) = \int_0^L \kappa \frac{\partial^2 \mathbf{X}(s,t)}{\partial s^2} \delta(\mathbf{x} - \mathbf{X}(s,t))\,\mathrm{d}s \qquad \forall \mathbf{x} \in \Omega,\ t \in]0,T[\tag{3}$$

$$\frac{\partial \mathbf{X}}{\partial t}(s,t) = \mathbf{u}(\mathbf{X}(s,t),t) \quad \forall s \in [0,L],\ t \in]0,T[\tag{4}$$

Here $\mathbf{u}$ is the fluid velocity and p is the fluid pressure. The problem is completely described once we fix boundary and initial conditions:

$$\mathbf{u} = 0 \qquad \text{on } \partial\Omega \times]0,T[\tag{5}$$

$$\mathbf{u}(\cdot,0) = \mathbf{u}_0(\cdot) \qquad \text{on } \Omega \tag{6}$$

$$\mathbf{X}(s,0) = \mathbf{X}_0(s) \quad \forall s \in [0,L]. \tag{7}$$

We observe that the choice of $\mathbf{F}$ is made in such a way that the motion of the boundary $\mathbf{X}$ is driven by its elastic

* Corresponding author. Fax: +39 (30) 371-5745;
E-mail: gastaldi@ing.unibs.it

Computational Fluid and Solid Mechanics 2003
K.J. Bathe (Editor)

energy (κ denotes the elasticity coefficient). For simplicity, we shall drop the convective term in Eq. (1) and consider the following variational form: given $\mathbf{u}_0 \in H_0^1(\Omega)^2$ and $\mathbf{X}_0 \colon [0,L] \to \Omega$, for almost every $t \in]0,T[$ find $(\mathbf{u}(t), p(t)) \in H_0^1(\Omega)^2 \times L_0^2(\Omega)$ and $\mathbf{X} \colon [0,L] \times]0,T[\to \Omega$, such that

$$\rho \frac{\mathrm{d}}{\mathrm{d}t}(\mathbf{u}(t),\mathbf{v}) + \mu(\nabla \mathbf{u}(t), \nabla \mathbf{v}) - (\nabla \cdot \mathbf{v}, p(t)) = \langle \mathbf{F}(t), \mathbf{v} \rangle \quad \forall \mathbf{v} \in H_0^1(\Omega)^2 \tag{8}$$

$$(\nabla \cdot \mathbf{u}(t), q) = 0 \quad \forall q \in L_0^2(\Omega)$$

$$\langle \mathbf{F}(t), \mathbf{v} \rangle = \int_0^L \kappa \frac{\partial^2 \mathbf{X}(s,t)}{\partial s^2} \mathbf{v}(\mathbf{X}(s,t))\,\mathrm{d}s \quad \forall \mathbf{v} \in H_0^1(\Omega)^2 \tag{9}$$

$$\frac{\partial \mathbf{X}}{\partial t}(s,t) = \mathbf{u}(\mathbf{X}(s,t),t) \quad \forall s \in [0,L], \tag{10}$$

$$\mathbf{u}(\mathbf{x},0) = \mathbf{u}_0(\mathbf{x}) \quad \forall \mathbf{x} \in \Omega, \tag{11}$$

$$\mathbf{X}(s,0) = \mathbf{X}_0(s) \quad \forall s \in [0,L],$$

$$\mathbf{X}(0,t) = \mathbf{X}(L,t), \quad \forall t \in [0,T]. \tag{12}$$

The well-posedness of problem presented in Eqs. (8)–(12) has been discussed in [6] for a one dimensional model.

We show a stability property for the solution of this problem as follows. Taking $\mathbf{v} = \mathbf{u}$ in Eq. (8), using Eq. (10), and integrating by parts, we have

$$\frac{\rho}{2}\frac{\mathrm{d}}{\mathrm{d}t}\|\mathbf{u}(t)\|_0^2 + \mu \|\nabla \mathbf{u}(t)\|_0^2 + \frac{\kappa}{2}\frac{\mathrm{d}}{\mathrm{d}t}\left\|\frac{\partial \mathbf{X}(t)}{\partial s}\right\|_0^2 \le 0. \tag{13}$$

The discretization of the problem under consideration is obtained with the introduction of suitable finite element spaces for the approximation of the evolution Stokes problem presented in Eq. (8), with a piecewise linear approximation of the boundary $\mathbf{X}$, and with a suitable computation of the load term in Eqs. (8), (9).

To this aim, we use the well-known $Q_2 - P_1$ Stokes element to approximate velocities and pressures in Eq. (8) and we integrate by parts Eq. (9), obtaining the following discrete scheme: for all $t \in]0,T[$, find $(\mathbf{u}_h(t), p_h(t)) \in \mathbf{V}_h \times Q_h$ and $\mathbf{X}_h(t) \in \mathbf{S}_h$ such that

$$\rho \frac{\mathrm{d}}{\mathrm{d}t}(\mathbf{u}_h(t),\mathbf{v}) + \mu(\nabla \mathbf{u}_h(t), \nabla \mathbf{v}) - (\nabla \cdot \mathbf{v}, p_h(t)) = \langle \mathbf{F}_h(t), \mathbf{v} \rangle_h \quad \forall \mathbf{v} \in \mathbf{V}_h \tag{14}$$

$$(\nabla \cdot \mathbf{u}_h(t), q) = 0 \quad \forall q \in Q_h$$

$$\langle \mathbf{F}_h(t), \mathbf{v} \rangle_h = -\int_0^L \kappa \frac{\partial \mathbf{X}_h(t)}{\partial s}^T D\mathbf{v}(\mathbf{X}_h(t)) \frac{\partial \mathbf{X}_h(t)}{\partial s}, \quad \forall \mathbf{v} \in \mathbf{V}_h \tag{15}$$

$$\frac{\mathrm{d}\mathbf{X}_{hi}}{\mathrm{d}t}(t) = \mathbf{u}_h(\mathbf{X}_{hi}(t),t) \quad \forall i = 1,\ldots,m \tag{16}$$

$$\mathbf{u}_h(\mathbf{x},0) = \mathbf{u}_{0h}(\mathbf{x}) \quad \forall \mathbf{x} \in \Omega, \tag{17}$$

$$\mathbf{X}_{hi}(0) = \mathbf{X}_0(s_i) \quad \forall i = 1,\ldots,m. \tag{18}$$

In Eqs. (14)–(18) the notation is as follows: $\mathbf{V}_h$ is the space of continuous piecewise biquadratic vectorfields vanishing on $\partial\Omega$; Q_h is the space of piecewise linear functions; $\mathbf{S}_h$ is the space used for the approximation of the boundary $\mathbf{X}$ and m is the dimension of $\mathbf{S}_h$. Finally, $D\mathbf{v}$ denotes the Jacobian matrix of the space derivatives of $\mathbf{v}$.

Remark 1 *We observe that the computation of $\mathbf{F}_h$ given in Eq. (15) is one of the main differences of our method from the one originally designed by Peskin. In particular, the variational formulation undergoing our finite element method allows us to compute $\mathbf{F}_h$ without introducing a discretization of the Dirac function. The integral in Eq. (15) can be easily evaluated using a quadrature formula.*

For the moment, we use a natural modification of the backward Euler scheme for advancing in time. Namely, our scheme consists in two steps: given the approximation $\mathbf{X}_h^n$ of $\mathbf{X}$ at time $n\Delta t$, we construct $\mathbf{F}_h^n$ and find the solution $(\mathbf{u}_h^{n+1}, p_h^{n+1})$ to the Stokes equations with the backward Euler method; then we move the immersed boundary, getting $\mathbf{X}_h^{n+1}$.

A comparison to different time approximation schemes will be the object of a future work.

3. Numerical results

Throughout this section Ω is the unit square $]0,1[\times]0,1[$, $L = 1$ and $T = 3$. If not stated otherwise, $\Delta t = 0.01$ (300 time steps), the domain Ω is partitioned in 32 by 32 subsquares and the immersed boundary $\mathbf{X}$ is approximated by using 160 points which are equally spaced in its parametric interval $[0,1]$.

In our first test the fluid is initially at rest and the curve $\mathbf{X}$ is initially the ellipsis centered at the barycenter of Ω, with the following parametric representation:

$$\mathbf{X}_0(s) = (0.5 + 0.25\cos(2\pi s), 0.5 + 0.1\sin(2\pi s)) \quad s \in [0,1].$$

The aim of this test is to examine the influence of the elastic force of the immersed boundary on the whole system.

In Fig. 1 we plot the evolution of the immersed boundary and the pressure p at the final time $T = 3$. As expected, the elastic force modifies the boundary towards its equilibrium configuration and induces a high pressure on the fluid in the interior of the boundary.

In order to show the robustness of our method, in Table 1 we report on the area of the region inside the immersed boundary at different time steps. It appears that in order to have reasonable results (with respect to the finite element mesh) it is advisable to have about two nodes of the boundary per element.

In the second test case, we check how the fluid drives the motion of the immersed boundary. To this aim, we position the initial immersed boundary as a circle centered at the middle of Ω with radius $1/4$. The initial fluid velocity is rotating clockwise. Since we are not considering

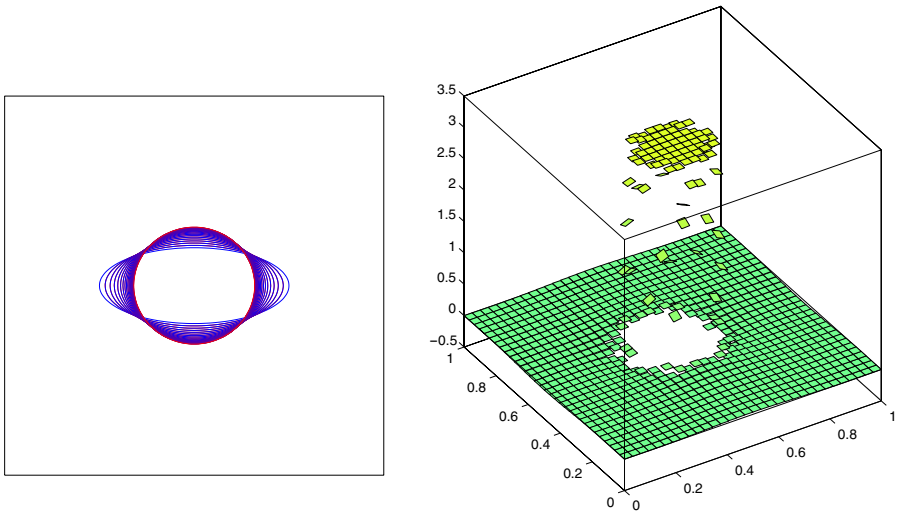

Fig. 1. The immersed boundary evolution (left) subjected to its elastic force and the final fluid pressure (right).

Table 1
Area loss with different values of m (points on the boundary) and N^2 (number of finite elements)

	m				
	20	40	80	160	320
$N = 8$	16.43	16.00	15.85	15.82	15.80
$N = 16$	12.92	5.77	5.42	5.32	5.29
$N = 32$	33.15	5.66	1.86	1.70	1.65

the convective term in the Navier–Stokes equation, we have to force the motion of the fluid by adding an extra term in the right hand side of Eq. (8). More precisely, we add a source term which would give a steady solution equal to $\mathbf{u}_0$ in absence of the immersed boundary.

In Fig. 2 we plotted the initial fluid velocity configuration together with the evolution of the immersed boundary. Since the boundary rotates and occupies almost the same position at every time step, we only plot the initial and final configurations and indicate in the picture with a triangle the motion of a fixed point of the curve. We have used a 32-by-32 mesh with $\Delta t = 0.01$ and 160 points for the boundary.

The final test takes into consideration the effects either of the elastic force of the immersed boundary and of the motion of the fluid. Namely, the initial $\mathbf{u}$ is as in the previous example (with the same extra load added to Eq. (8)) and the initial configuration of the curve $\mathbf{X}$ is given by an ellipsis located in the left bottom part of Ω. We plot in Fig. 3 the evolution of the boundary and the final velocity field computed with a 32-by-32 mesh with $\Delta t = 0.01$ and 160 points for the boundary. For graphical reasons, we plot the $\mathbf{u}$ on a 16-by-16 mesh.

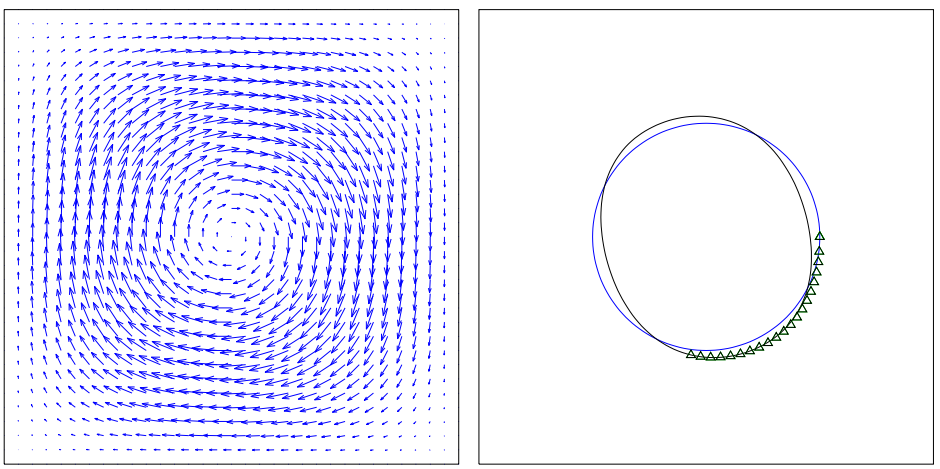

Fig. 2. A circle driven by a rotating fluid: the initial fluid (left) and the evolution of $\mathbf{X}$ (right).

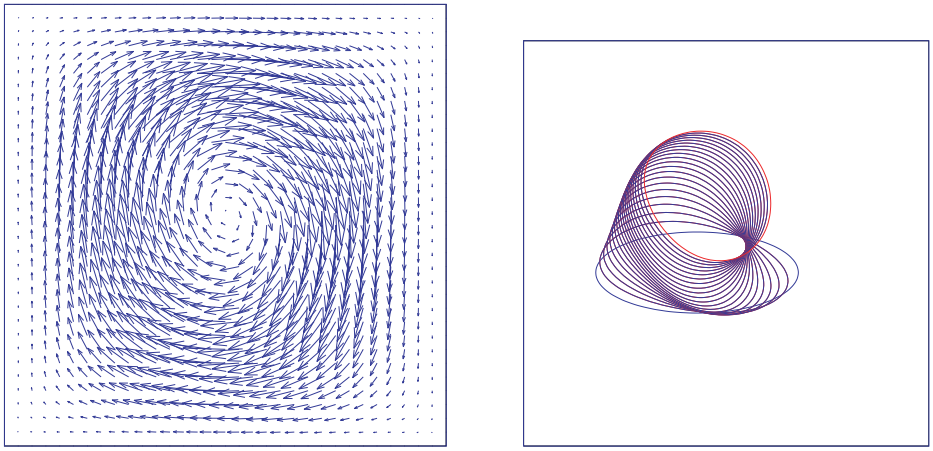

Fig. 3. An ellipsis driven by a rotating fluid: the initial fluid (left) and the evolution of **X** (right).

References

[1] Peskin CS. The immersed boundary method. In: Acta Numerica, 2002, Vol 11. Cambridge University Press, 2002, pp. 479–517.

[2] Bathe KJ, Zhang H, Ji S. Finite element analysis of fluid flows fully coupled with structural interactions. Comput Struct 1999;72:1–16.

[3] Zhang H, Bathe KJ. Direct and iterative computing of fluid flows fully coupled with structures. In: Bathe KJ (Ed), Computational Fluid and Solid Mechanics. Proceedings of the First MIT Conference on Computational Fluid and Solid Mechanics. Amsterdam: Elsevier Science, 2001.

[4] Rugonyi S, Bathe KJ. On the finite element analysis of fluid flow fully coupled with structural interactions. Comput Model Eng Sci 2001;2:195–212.

[5] Quarteroni A. Modeling the cardiovascular system: a mathematical challenge. In: Engquist B, Schmid W (Eds), Mathematics Unlimited – 2001 and Beyond. Berlin: Springer, 2001, pp. 961–972.

[6] Boffi D, Gastaldi L. A finite element approach for the immersed boundary method. Comput Struct 2003, to appear. Special issue in honor of K.J. Bathe.

[7] Peskin CS, Printz BF. Improved volume conservation in the computation of flows with immersed elastic boundaries. J Comput Phys 1993;105(1):33–46.

[8] Lai M-C, Peskin CS. An immersed boundary method with formal second-order accuracy and reduced numerical viscosity. J Comput Phys 2000;160(2):705–719.